DESIGN OF A MULTI-BAND FRACTAL ANTENNA

By

TRAN THI MY DUNG

FINAL PROJECT REPORT

Submitted to the Electrical & Electronics Engineering Programme
in Partial Fulfillment of the Requirements
for the Degree
Bachelor of Engineering (Hons)
(Electrical & Electronics Engineering)

Universiti Teknologi Petronas
Bandar Seri Iskandar
31750 Tronoh
Perak Darul Ridzuan

CERTIFICATION OF APPROVAL

DESIGN OF A MULTI-BAND FRACTAL ANTENNA

by

Tran Thi My Dung

A project dissertation submitted to the
Electrical & Electronics Engineering Programme
Universiti Teknologi PETRONAS
in partial fulfilment of the requirement for the
Bachelor of Engineering (Hons)
(Electrical & Electronics Engineering)
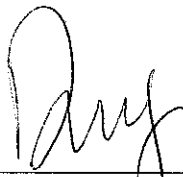
Approved:

_____

Assoc. Prof. Varun Jeoti
Project Supervisor

UNIVERSITI TEKNOLOGI PETRONAS

TRONOH, PERAK

June 2007

CERTIFICATION OF ORIGINALITY

This is to certify that I am responsible for the work submitted in this project, that the original work is my own except as specified in the references and acknowledgements, and that the original work contained herein have not been undertaken or done by unspecified sources or persons.

Tran Thi My Dung

ABSTRACT

In recent years, the demand for compact and multi-function handheld communication devices has grown significantly. Devices having internal antennas have appeared to fill this need. Antenna frequency band and size are major factors. In the past few decades, fractal antenna theory develops rapidly, basing on fractal geometry to maximize the length of material. Fractal surface is a function of roughness, by increasing roughness, polarization changes. For this reason, fractal antennas are very compact, are multi-band and have useful applications which require small, cheap and effective antenna such as cellular telephones and microwave communications.

A notable fractal antenna to be mounted on wireless devices such as mobile phones, laptops is presented in this thesis. The proposed multi-band fractal antenna simultaneously operates in the IEEE 802.11a, IEEE 802.11b/g and WiMax frequency bands. The multi-band behavior is obtained by using Sierpinski Gasket fractal structures. The overall size of the antenna renders it suitable to be installed at the back of the mobile phone or the top of the display of a notebook. Simulation results are obtained by CST Microwave studio.

ACKNOWLEDGEMENTS

With the help and support from many people while working on this project, I would like to relish this opportunity to express my gratitude to all who helped me to complete this work

First of all, I would like to thank Associate Professor Dr. Varun Jeoti from Electrical and Electronics Engineering Department, Universiti Tecknologi Petronas, the project supervisor who has been given many supportive and constructive guidance and advices. His suggestions have guided me throughout this project.

I also acknowledge Mr. Adz Jamros Bin HJ Jamali for his assistance in the Communication lab.

TABLE OF CONTENTS

LIST OF FIGURES

CHAPTER 1

INTRODUCTION

1.1 Overview

The major part of the literature is dealing with compact monopole microstrip antenna with fractal shape. The reasons that made this configuration popular for wireless applications are easy in manufacturing and its small size. However with more requirements, more frequency operations inside one wireless device make the field of multi-frequency antennas for wireless applications an open challenge. The solution to the need of multi-band behavior can be fulfilled by applying fractal concepts on antenna designing.

Fractal shaped antennas have already been proved to have some unique characteristics that are linked to the geometrical properties of fractals. The self-similarity property of fractals makes them especially suitable to design multi-frequency antennas. The thesis is aimed to present a new multi-band single-feed fractal antenna for WLAN and WiMax applications, operating in the IEEE 802.11a (5725-5825MHz), IEEE 802.11b/g (2400-2484MHz) and IEEE 802.16 (3.5MHz) frequency band.

1.2 The thesis organization

In this thesis, Chapter 2 summarizes about the related literature concepts from which the problem statement and the objectives of my project are drawn. All of chapter 3 devotes to describe the project methodology which includes the task flow of whole project and the method used to design and simulate the proposed antenna. Chapter 4 gives the detail results about the proposed antenna performance in CST simulation

and some discussion involved to those results. At the end of chapter 4, some modifications are proposed in order to reduce the size of the antenna. And the last chapter, chapter 7 will draw some conclusions and recommendations about the overall project.

CHAPTER 2
LITERATURE REVIEW

2.1 Antenna

The IEEE Standard Definitions of Term for Antennas (IEEE Std 145-1983) defines the antenna as 'a means for radiating or receiving radio wave'. In other words, antenna is an electrical device which converts between electrical and electromagnetic energy. It is well known that there is a strong relationship between the performance of an antenna and its size, relative to the operating wavelength. Antennas are usually designed to operate over a small frequency band (or narrowband).

2.2 Radiation Mechanism

Based on the fundamental electromagnetic theory, to create radiation, there must be a time-varying current or an acceleration (or deceleration) of charge. To create charge acceleration, the wire must be bent, curved, and discontinuous or terminated (because the charges is moving inside a wire, by changing direction of road, charges have to accelerate or decelerate). In conclusion, if the charge is not moving, current is not created, and thus there is no radiation. If the charge is moving with constant velocity, there is no radiation if the wire is straight and infinite in length, unless the wire is bent, curved, discontinuous or terminated. If the charge is oscillating in time motion (mean the current changes with time), it radiates even the wire is straight.

Studying for radiation mechanism is more specific on dipole antenna. Assume that the voltage source is sinusoidal. Because of electric force, one pole of antenna will become a positive charge; meanwhile the other is a negative charge. When the applied voltage is in positive cycles and increasing, the electric intensity will goes

3

from positive to negative charge. When the applied voltage is in positive cycles and decreasing, the electric intensity will goes in opposite direction that means it goes from negative to positive charge. When the applied voltage is in negative cycle, the process is inverted [4].

Because the applied voltage is changing, leading the current changing, thus the electric intensity is changing. Therefore the magnetic field is created, and varying. This varying magnetic field will created an electric field around. That is the way how antenna radiates.

2.3   Antenna parameters

There are some essential parameters of an antenna, such as radiation patterns, radiation pattern lobe, field region, radiation power density, radiation intensity, directivity, gain, beam efficiency and polarization [5].

Antenna pattern is defined as a graphical representation of the radiation properties of the antenna as the mathematical function of space coordinates. The function concerned is a function of the observer's position along a path with constant radius from the antenna. The radiation properties consist of power flux density, radiation intensity, field strength, directivity phase or polarization...The used coordinator system include azimuth plane which is the plane of x and y, with the angle from positive x to positive y, elevation plane which perpendiculars to azimuth plane and contains z axis. The θ elevated angle is calculated from positive z to negative z.

Radiation lobe is a portion of radiation pattern bounded by regions of relatively weak radiation intensity. From radiation lobe, the direction of maximum radiation can be determined.

The space surrounding an antenna is usually divided into 3 **filed regions** which are reactive near field, radiating near field, and far field. The field boundary depends on the physical dimension of the antenna and the wavelength. For most antennas, R1, R2 is calculated by [4]:

4

$$R1 = 0.62 \ D^3/\lambda$$

$$R2 = 2D^2/\lambda$$

In practice, the far-field region is much in concern, since the using purpose of an antenna is to transfer signal through some distances.

The region surrounding antenna is described in the below figure.
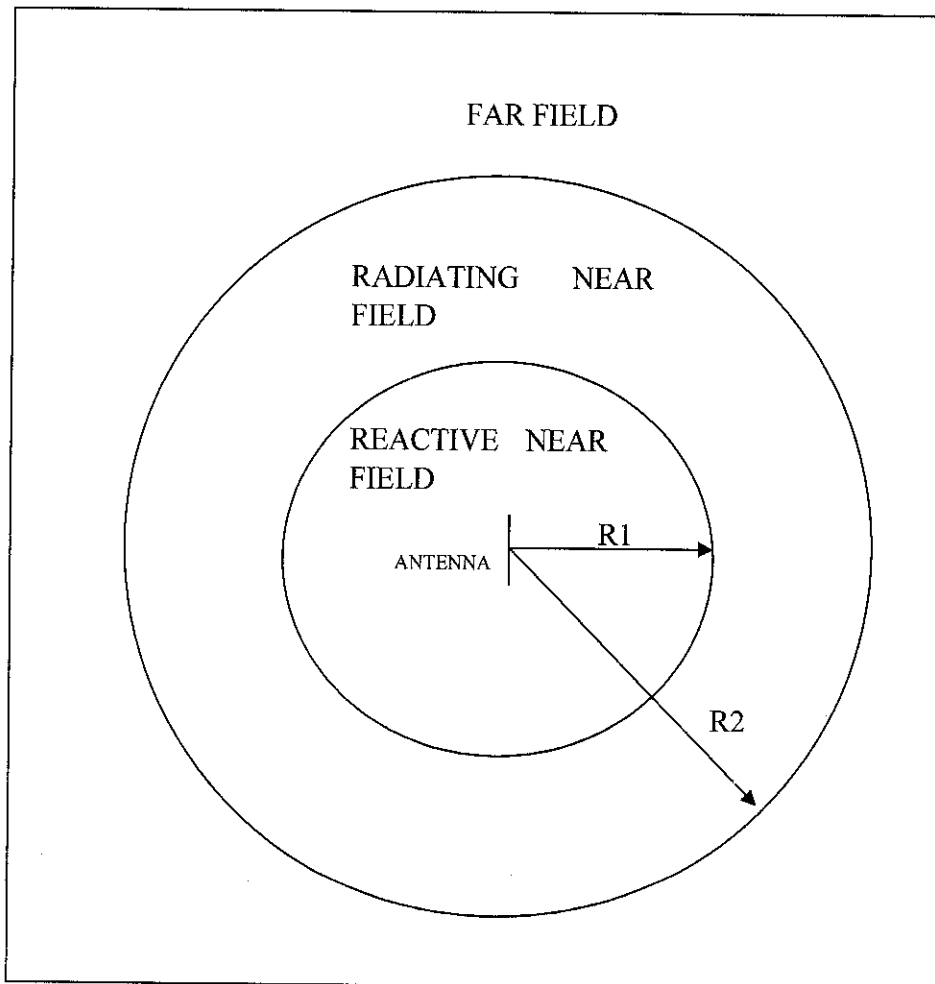
Figure 2. 1 Field region of an antenna

From electromagnetic theory, the power density of electromagnetic field is the Poynting vector of E (electric field) and H (magnetic field). Therefore, **radiation power density** at a certain point is W = E x H. Since the Poynting vector is a power

density W, the total power P_{rad} crossing a closed surface can be obtained by integrating the normal component of the Poynting vector over the entire surface.

$$P_{rad} = W_{rad}.ds$$

Radiation intensity U in a given direction is the power radiated from an antenna per unit angle.

$$U = \frac{P_{rad}}{4\pi} = \frac{SW_{rad}}{4\pi} = r^2 W_{rad}$$

Where S is the surface area of total radiated sphere

The directivity of an antenna is the ratio of the radiation intensity in a given direction (θ, α) from the antenna to the radiation intensity averaged over all directions.

$$D(\theta, \alpha) = \frac{U(\theta, \alpha)}{U_0}$$

With $U_0 = \frac{P_{rad}}{4\pi}$

So $D(\theta, \alpha) = 4\pi \frac{U(\theta, \alpha)}{P_{rad}}$

Gain of an antenna is used to measure its performance. It depends on the efficiency of the antenna as well as the directional capabilities while directivity is a measure that describes only the directional properties. The absolute gain of an antenna (in a given direction) is defined as the ratio of the radiation intensity, in given direction, to the radiation intensity that would obtained if the power accepted by the antenna were radiated isotropically.

$$Gain = \frac{U(\theta, \alpha)}{U_{iso}} = 4\pi \frac{U(\theta, \alpha)}{P_{in}}$$

6

Added to that, the total radiated power: $P_{rad} = \eta \, P_{in.}$

Where η is the antenna radiation efficiency

$$So \; Gain = \frac{U(\theta, \alpha)}{U_{iso}} = 4\pi \frac{U(\theta, \alpha)}{P_{in}} = 4\eta\pi \frac{U(\theta, \alpha)}{P_{rad}} = \eta D(\theta, \alpha)$$

Therefore in case of lossless antenna, Gain (θ, α) = D (θ, α)

Total antenna efficiency, η is used to cake into account losses at the input terminals and within the structure of the antenna. Such looses may be due, for example, reflections because of the mismatch between the transmission line and the antenna and I^2R losses (conduction and dielectric).

Beam efficiency is used to judge the quality of transmitting and receiving antennas. The **bandwidth** of an antenna is defined as the range of the frequencies within which the performance of the antenna is acceptable.

2.4   Method of Analysis

There are many methods of analysis for microstrip antennas. The most popular methods are the transmission line and cavity.

2.4.1   Transmission line method

Transmission line method concerns to fringing effects. Because the dimensions of the patch are finite in length and width, the fields as the edges of the patch undergo fringing. The amount of fringing is depended on the dimensions of the antenna and the height of substrate. The fringing effect is inversely proportional to the ratio length/height or width/height. The fringing effect makes the microstrip look wider electrically compared to its physical dimensions. Therefore the effective dielectric

constant ε_{reff} and extended distance ΔL are introduced to account for fringing effect. Some useful formulas in rectangular antenna design are [5][6]:

The width:

$$W = \frac{v_0}{2 f_r} \sqrt{\frac{2}{\varepsilon_r + 1}}$$

The effective dielectric constant

$$\varepsilon_{reff} = \frac{\varepsilon_r + 1}{2} + \frac{\varepsilon_r - 1}{2} \left[1 + 12 \frac{h}{W} \right]^{-1/2}$$

The extend of length

$$\Delta L = 0.412 \frac{(\varepsilon_{reff} + 0.3) \left(\frac{W}{h} + 0.264 \right)}{(\varepsilon_{reff} - 0.258) \left(\frac{W}{h} + 0.8 \right)} h$$

Since the effective length in microstrip antenna is chosen to be $L_{eff} = \frac{\lambda}{2}$ therefore the actual length is:

$$L = \frac{\lambda}{2} - 2\Delta L$$

Where:

f_r is resonant frequency

h is the height of the substrate

8

λ is wave length of the resonant frequency in ε_{reff} environment.

v_0 is the velocity of wave in free space environment.

2.4.2 Cavity method

Cavity model is one of method to assess antenna behavior, and it is usually used to measure microstrip antenna. A cavity is defined as a thing which is bounded by electric conductors (electric wall) and has a magnetic wall along perimeter of the patch. A cavity has a main advantage, it not radiate any power, its input impedance is purely reactive, no R_r, R_L, which make calculations complicating. Therefore, if the antenna can be considered as a cavity, the calculation will become much easier.

If L> W> h, the mode is TM_{010}^{x} whose the frequency is given by:

$$(f_r)_{010} = \frac{v_0}{2L\sqrt{\varepsilon_r}}$$

If L> W> L/2>h, the mode is TM_{001}^{x} whose the frequency is given by:

$$(f_r)_{001} = \frac{v_0}{2W\sqrt{\varepsilon_r}}$$

If L>L/2> W> h, the mode is TM_{020}^{x} whose the frequency is given by:

$$(f_r)_{020} = \frac{v_0}{L\sqrt{\varepsilon_r}}$$

If W> L > h, the dominant mode is the TM_{001}^{x}.

9

2.5 Microstrip antenna

Microstrip antenna consists of a radiating patch on one side of a dielectric substrate, which has a ground plane on the other side. All microstrip can be divide into three basic categories: microstrip patch antennas, microstrip dipoles, printed slot antennas.

Microstrip patch antenna consists of a conducting patch in both side of a dielectric surface. Microstrip dipole antenna consists of a folded dipole combined with another similar dipole. Printed slot antennas comprise a slot in the ground plane of a grounded substrate.

Radiation from a microstrip antenna can be determined from the field distribution between the patch metallization and ground plane. Alternatively, radiation can be described in terms of the surface current distribution on the patch metallization. All obey the Maxell's equations.

There are many techniques models have been used to determine microstrip antenna characteristics such as the transmission model, generalized model, cavity model, and multi port network model.

Another important issue in antenna design is feeding technique selection. Selection of the feeding technique is governed by a number of factors. The most important is impedance matching between radiating structure and feed structure. Others are bends, stubs, junctions, transitions…which influences radiation and surface wave loss.

Microstrip patch antennas are increasing in popularity for use in wireless applications due to their low-profile structure. Therefore they are extremely compatible for embedded antennas in handheld wireless devices such as cellular phones, pagers, etc... Some of their principal advantages and disadvantages are [1]:

Advantages

- Light weight and low volume.

- Low profile planar configuration which can be easily made conformal to host surface.

- Low fabrication cost, hence can be manufactured in large quantities.

- Supports both, linear as well as circular polarization.

- Can be easily integrated with microwave integrated circuits (MICs).

- Capable of dual and triple frequency operations.

- Mechanically robust when mounted on rigid surfaces.

Disadvantages

- Narrow bandwidth

- Low efficiency

- Low Gain

- Extraneous radiation from feeds and junctions

- Low power handling capacity.

- Surface wave excitation

2.6   Multi-band Antenna

Multi-band Antenna, as the name, is able to work effectively in many different frequency bands. Nowadays, multi-band antennas become very popular. For example,

with the widespread use of the GSM system which employs the dual frequency bands of 900 and 1800 MHz, multi-band operation of mobile phones is advancing rapidly. As things stand today, the application of multi-band systems with a variety of frequency band combinations is accelerating, the communications capacity is increasing and new functions are being added including GPS (1.57 GHz), Bluetooth (2.4 GHz), WiMax (3.5 GHz), WiFi (5.8 GHz)...

2.7   Fractal antenna

Fractal geometries have found an intricate place in science as a representation of some of the unique geometrical features occurring in nature. For example, fractals are used to describe the branching of tree leaves and plants, the sparse filling of water vapor that forms clouds, the random erosion that carves mountain faces, the jaggedness of coastlines, or the nature of noise...
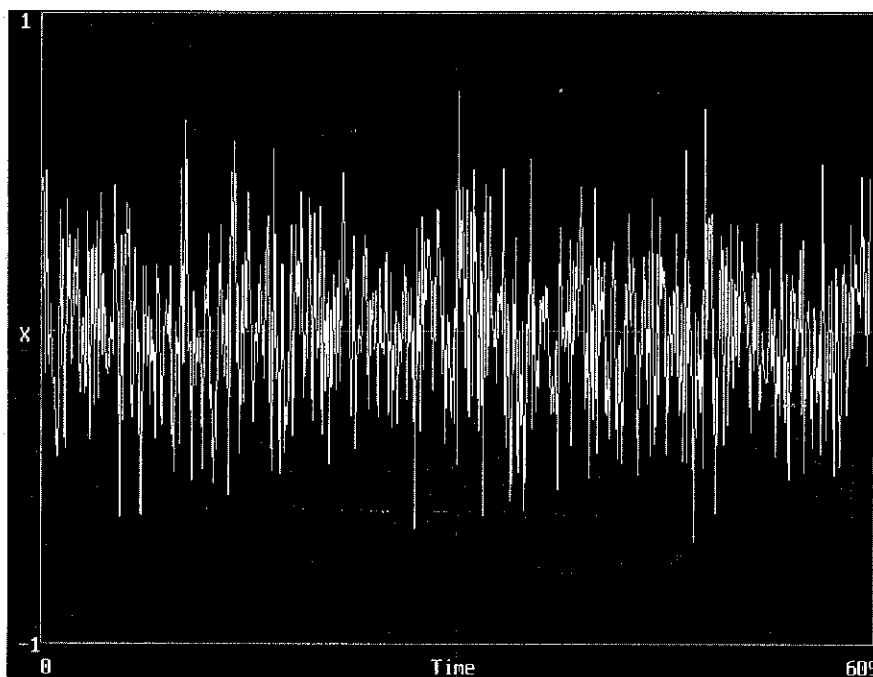

Figure 1   Noise signal

Let take the example from the noise signals to illustrate the fractal concepts, they appear irregular, yet have underlying order, and possess structure on all scales (fig.1).

A noise signal looks like a rough and jagged curve when viewed in 200 seconds. When viewed by 1 second, the noise again appears as a rough, jagged curve, and it retains this appearance even much shorter or longer time. This similar structure at many different scales is a characteristic of fractals. Whether a fractal set has statistical or exact self-similarity, its similar appearance on all scales suggests that the set might be best constructed through recursive or iterative means. This stands in contrast to Euclidean structures, which may be more easily defined using formulae. One example of a Euclidean structure, a beach ball looks like a point if seen from outer space, a sphere when view by person on land. Therefore the substantially different appearance when view in different scales is considered as Euclidean structures. The table 1 summarizes some qualitative differences between fractal and Euclidean geometry [2]:

Fractal geometry	Euclidean Geometry
Often defined by iterative rule	Often defined by formulae
Structure on many scales	Structure on one or few scales
Dilation symmetry (self-similarity)	No self similarity
Fractional dimension possible	Integer dimension
Long range correlation	Variable correlation
Described as ramified, variegated, spiky	Described regular
Rough on most scales	Smooth on most scales

Table 1   Contrast summary of Fractal and Traditional Euclidean Geometrical attributes.

In the study of antennas, fractal antenna theory is a relatively new area. The fractal design of antennas results from the combination between classical electromagnetic

theory and fractal geometry (figure 2).
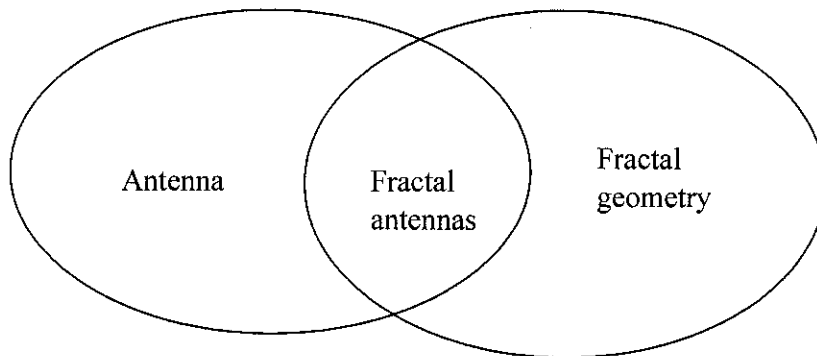
Figure 2   Fractal Antenna

Fractal structures with a self-similar geometric shape consisting of multiple copies of themselves on many different scales have therefore the potential to be frequency-independent or at least multi- frequency antennas. Therefore a fractal antenna is defined as an antenna that uses a self-similar design to maximize the length, or increase the perimeter (on inside sections or the outer structure), of material that can receive or transmit electromagnetic signals within a given total surface area. Examples of classical fractals are the Cantor set, the Koch curve, the Sierpinski gasket and carpet, the Peano curve, the Hilbert curve, and many more [3].

Figure 3   The Sierpinski gasket structure

Figure 4   The Koch curve structure

14

There are some significant milestones in fractal antenna development [4]:

- 1986-1993. several authors theoretically investigate the relationships between fractal arrays and their array factors. Some fractal and array properties such as Fractal Dimension and Secondary Lobe Ratio are linked for the first time.

- 1993, November. The potentiality of fractal arrays to become multi-frequency arrays is introduced by C.Puente at the University of Illinois at Urbana-Champaign during a graduate course discussion.

- 1994. Some preliminary ideas on multi-band fractal arrays are presented by C.Puente at an URSI meeting in Las Palmas, Gran Canaria, Spain. Further work on such ideas gives place to a paper that is submitted to the IEEE Transactions on Antennas and Propagation in May 1994, and published in May 1996.

- 1995, May. After several months working on the invention of the Sierpinski antenna, the Universitat Politècnica de Catalunya finally applies for the patent on Fractal and Multi-fractal Antennas. Such results proved the feasibility of fractals to become multi-band antennas

- 1995. Summer. Some preliminary ideas on fractal small antennas are suggested by N.Cohen from the Boston University.

- 1996-1998. The first reported experimental results on fractal multi-band antennas are published by the Electromagnetic & Photonics Engineering research team from the Universitat Politècnica de Catalunya.

- 1998. The Koch monopole becomes the first reported fractal small antenna that improves the features of some classical antennas in terms of bandwidth, resonance frequency and radiation resistance. Whether such antennas are bounded to the fundamental limits on small antennas is still a topic under investigation.

- 1998. The Fractal Team from the Electromagnetics & Photonics Engineering group (UPC), in cooperation with Fractus^{TM} the Fractal Antennas^{TM} Company from the Sistemas Radiantes F.Moyano S.A. group, developed the first commercial multi-band fractal shape antennas for GSM + DCS cellular phone systems.

Fractal antennas have some advantages than other classical antennas such as: multi band, more effective, greater input resistance, improve directivity…Of course with the structure of fractal geometry, fractal antennas are allowed to operate with multi radio frequencies. Moreover fractal antennas are effective antennas. Fractal antennas are convoluted, uneven shapes and sharp edges, corners, and discontinuities tend to enhance radiation of electromagnetic energy from electric systems. Fractal antennas have therefore the potential to be efficient. This is particularly interesting when small antennas are to be designed, since small antennas are not generally good at radiating electromagnetic energy. Fractal antennas provide greater input resistance comparing to same size traditional antennas. Some fractals have the property that they can be very long but still fit in to a certain volume or area. Since fractals do not have a dimension that is an integer, for example it can be something between a line and a plane; they can more effectively fill some volume or area.

There are many applications that can benefit from fractal antennas. For example, compact integrated antennas are used in personal hand-held wireless, multi functions devices such as supporting GSM, Bluetooth, wireless LAN in cell phones, laptops and PDAs... Fractal antennas can also enrich applications that include multi-band transmissions such as GPS services or the global positioning satellites. Fractal antennas also decrease the area of a resonant antenna, which could lower the radar cross-section (RCS). This benefit can be exploited in military applications [3].

2.8   Sierpinski gasket fractal antenna behavior

There are quite a lot of fractals named after Waclaw Sierpinski, a Polish mathematician who lived from 1882 to 1969. These include the Sierpinski Triangle, the Sierpinski Carpet, the Sierpinski Pyramid (the 3D version of the Sierpinski

Triangle) and the Sierpinski Cube (the 3D version of the Sierpinski Carpet). The 2D figures will be described here, Sierpinski Triangle. The traditional Sierpinski Triangle, also called Sierpinski Gasket and Sierpinski Sieve, can be drawn as following rules: The Sierpinski triangle fractal is made by drawing three lines that connect the midpoints of the triangle's sides. The results are a centre white triangle shown in the figure. The original triangle is now divided into three smaller triangles. The above step is repeated for each triangle. A geometric method of creating the gasket is to start with a triangle and cut out the middle piece as shown in the generator below. This results in three smaller triangles to which the process is continued. The nine resulting smaller triangles are cut in the same way, and so on, indefinitely (fig.5, [5]).
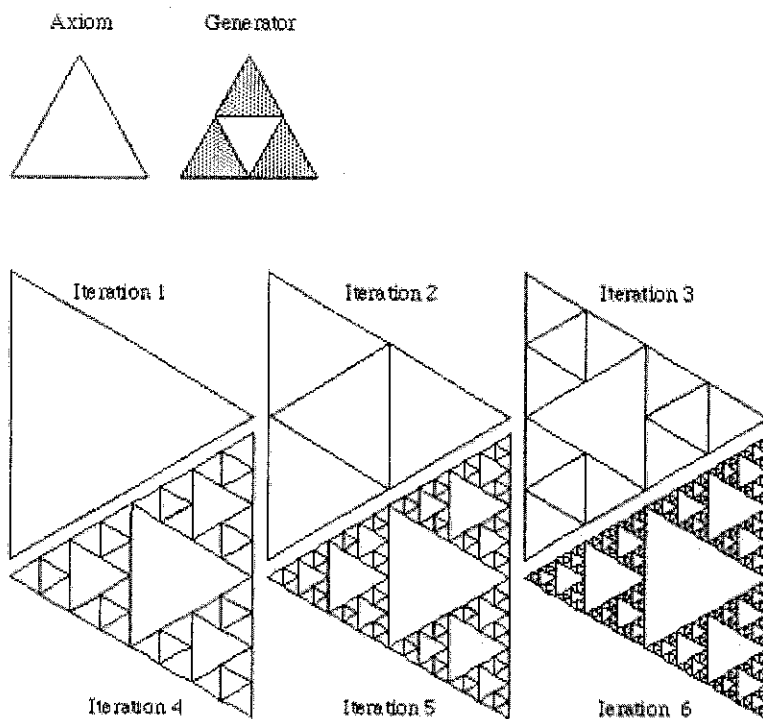

Figure 5   The Sierpinski generator and its iterations

Thus the gasket is perfectly self similar, an attribute of many fractal images. Any triangular portion is an exact replica of the whole gasket. The fractal dimension of the

gasket is D = log 3 / log 2 = 1.5849, ie: it lies dimensionally between a line and a plane.

A particular interest is the area of the holes and the circumference of the solid pieces. If the area of the original triangle is 1 then the first iteration removes 1/4 of the area. The second iteration removes a further 3/16 and the third a further 9/64. The total area removed after the Nth iteration is given by [5]

$$A_N = \frac{1}{3} \sum_{i=1}^{N} \left(\frac{3}{4}\right)^i \qquad\qquad A_\infty = 1$$

If the circumference of the original triangle is 1 then after the first iteration the circumference increases by 1/2. After the second iteration it increases by 3/4. The circumference after the Nth iteration is given by [5]

$$C_N = 1 + \frac{1}{3} \sum_{i=1}^{N} \left(\frac{3}{2}\right)^i \qquad\qquad C_\infty = \infty$$

The resonant frequencies of the traditional Sierpinski gasket can be fully determined if the height, the flare angle and the transformation are known. The first resonance occurs when the perimeter of the Sierpinski triangle is slightly more than half a wavelength [6], [7]. The second resonance is spaced by a factor of approximately 3.5 from the first one independently from the transformation [7]. The bands from the second and above are log-periodically spaced by a factor which is determined by the iterative construction procedure.

It is interesting to notice that the bands are log-periodically spaced by a factor δ of 2, which exactly the characteristic scale factor that relates the several gasket sizes within the fractal shape. The number of band is directly associated with the number of fractal iteration stages. From the band location and the height to wavelength ratio numbers, the frequency design equation for the Sierpinski monopole is [8]:

$$f_n = 0.26 \times \frac{c}{h} \delta^n$$

Where c is the vacuum speed of light, h is the height of the largest gasket, and δ is the log-period. For the traditional Sierpinski gasket, δ is 2.

2.9 Problem statement

The rapid expansion of wireless technology during the last years has set new demands on integrated components including the antennas. Today the trend of microwave device design is to bend the best of high fashion with the best of high technology. For example of cell phone, a cell phone nowadays does not only work as the phone, capable of delivering best quality of voice and data transmission, but also operate in multiple radio frequency such as GSM, WCDMA, Bluetooth, or WiFi radio, WiMax... for other services. Those raise two main development trends for antenna design, compact and multi-band antennas. Therefore with their advanced features like multi-band behavior, small size, fractal antennas become very potential antennas in future.

2.10 Objectives and study scopes

This project involves different disciplines such as electromagnetic field theory, numerical methods, antenna theory and fractal geometry. The project has been lasting for two semesters. Since time limitation, the project focused on the antenna theory and fractal shape study, which was conducted in the first semester and fractal antenna design in the second semester. The proposed antenna should operate in three different bands of frequency which are IEEE 802.11a (5725-5825MHz), IEEE 802.11b/g (2400-2484MHz) and IEEE 802.16 (3.5GHz).

CHAPTER 3

METHODOLOGY

3.1 Project task flow

This final year project lasts for two study semesters and focuses on understanding antenna, antenna design concepts, CST software in the first semester and then designing an effective multi-band fractal antenna in the other semester.

The work firstly focused on antenna theory including its characteristics and parameters, and microstrip antenna. At the same time, CST software training was conducted. After understanding that basic knowledge, a rectangular microstrip antenna was constructed by CST software and simulated to verify theory.

In the second semester, a fractal antenna is designed basing on antenna theory and fractal theory. The results were analyzed and some modifications were made for better overall performances.
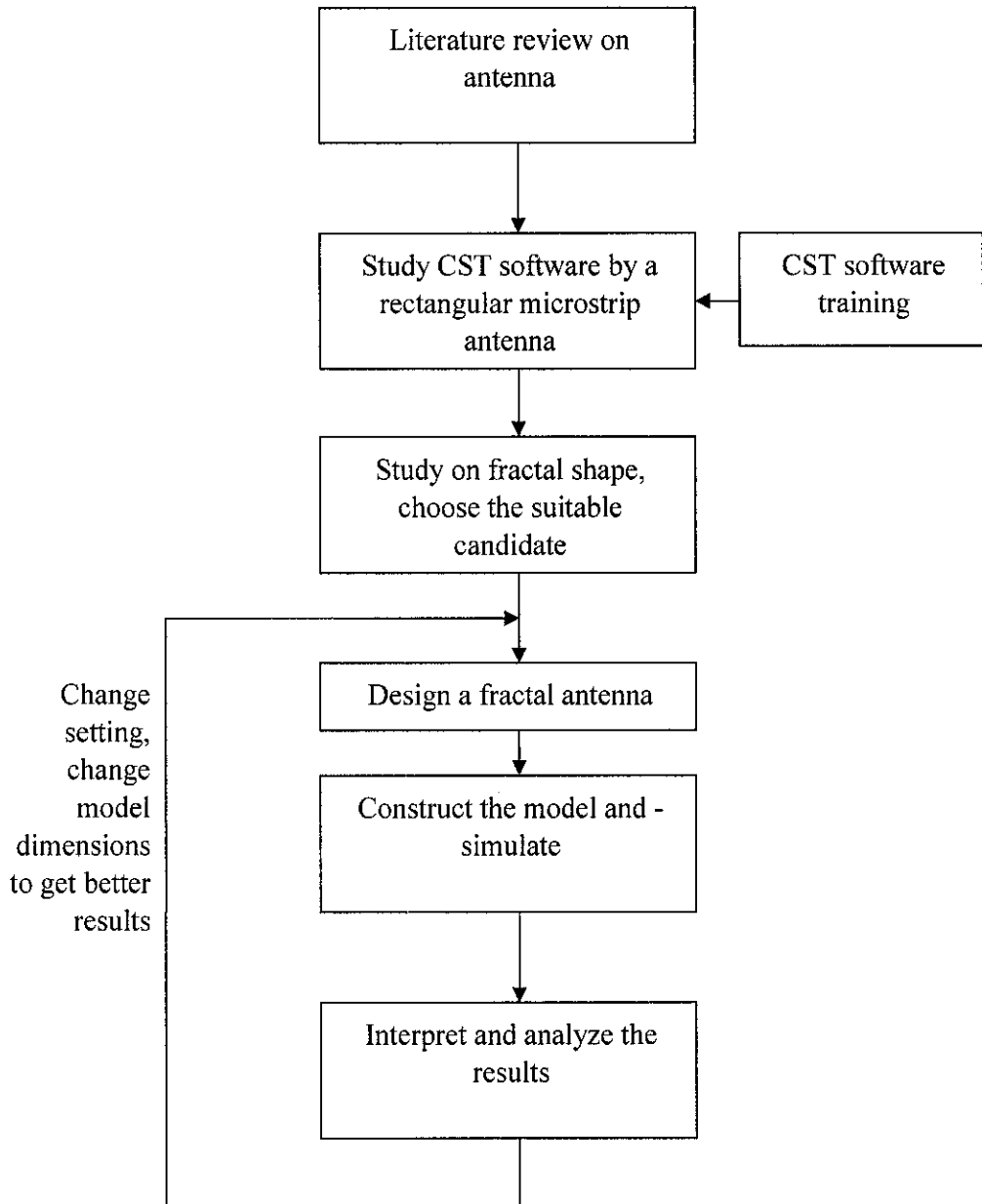
```
            ┌─────────────────────┐
            │  Literature review on │
            │       antenna         │
            └──────────┬──────────┘
                       │
                       ▼
            ┌─────────────────────┐        ┌──────────────┐
            │  Study CST software by a │◄───│ CST software │
            │  rectangular microstrip  │    │   training   │
            │       antenna         │        └──────────────┘
            └──────────┬──────────┘
                       │
                       ▼
            ┌─────────────────────┐
            │  Study on fractal shape, │
            │  choose the suitable  │
            │      candidate        │
            └──────────┬──────────┘
                       │
      ┌────────────────┤
      │                ▼
Change │        ┌─────────────────────┐
setting,│       │  Design a fractal antenna │
change │        └──────────┬──────────┘
model  │                   │
dimensions│                ▼
to get better│     ┌─────────────────────┐
results │        │  Construct the model and - │
        │        │       simulate        │
        │        └──────────┬──────────┘
        │                   │
        │                   ▼
        │        ┌─────────────────────┐
        │        │  Interpret and analyze the │
        │        │       results         │
        │        └──────────┬──────────┘
        └───────────────────┘
```

Figure 6   Project process flow

3.2   The fractal Sierprinski antenna design

The restriction though for printing the traditional Sierpinski gasket monopole on portable wireless devices has been its large physical size, which is imposed by the fact that the spacing between its first two bands is in the order of 3.5 regardless of the similarity factor. The Sierpinski gasket monopole antenna is constructed by applying a geometric transformation on the triangular monopole antenna of Fig 4.
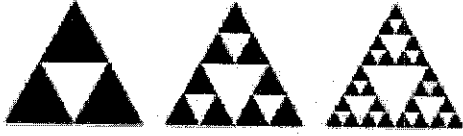
21

Figure 7   The Sierpinski gasket structure

Thus, for the traditional Sierpinski configuration the first pair of controllable bands is the second and third one and so fourth.

Added to that, the first resonance occurs when the perimeter of the Sierpinski triangle is slightly more than half a wavelength. The second resonance is spaced by a factor of approximately 3.5 from the first one independently from the transformation. The bands from the second and above are log-periodically spaced by a factor which is determined by the iterative construction procedure. In case of similarity transformation this factor is 2, while in case of affine transformation this factor can be altered in order to allocate the bands of interest. Since the 3.5 spacing between the first two bands cannot be controlled they cannot be used for band allocation.

Among three intended frequency bands (2.4GHz, 3.5 GHz, 5.8GHz), the lowest frequency is 2.4GHz. This 2.4GHz frequency should be allocated in the second band. Therefore the first frequency band should be 2.4/3.5 = 0.686 GHz. This frequency corresponds by the antenna structure, when the perimeter of the Sierpinski triangle is slightly more than half a wavelength. The frequency design equation for the Sierpinski monopole is [8]:

$$f_n = 0.26 \times \frac{c}{h} \delta^n$$

Where c is the vacuum speed of light, h is the height of the largest gasket, and δ is the log-period. For the traditional Sierpinski gasket, δ is 2.

22

The wavelength corresponds to frequency of 0.686GHz is:

$$\lambda = \frac{3 \times 10^8}{0.686 \times 10^6} = 437.32 m$$

Hence the perimeter of the Sierpinski triangle is equal to:

$$p = \frac{\lambda}{2} = \frac{437.32}{2} = 218.66 mm$$

Each side of the Sierpinski triangle is 218.66/3 = 72.89mm

Therefore the height of the Sierpinski triangle is:

$$h = \frac{72.89 \times \sqrt{3}}{2} = 63.12 mm$$

From the equation $f_n = 0.26 \times \frac{c}{h} \delta^n$

$$\frac{f_{n+1}}{f_n} = \frac{\delta^{n+1}}{\delta^n} = \delta$$

The next frequency is 3.5 GHz, the radio is 3.5G/2.4G = 1.458 = δ

Hence $\frac{1}{\delta_1} = \frac{1}{1.4} = 0.686$, so the height of sub-triangle is $h_1 = \frac{h}{\delta_1} = 0.686 \times h$

By the same procedure, the height of the second sub-triangle, which corresponds to 5.8 GHz frequency, is:

$$h_2 = \frac{h_1}{\delta_2} = h_1 \times \frac{3.5G}{5.8G} = h \times 0.686 \times 0.603 = h \times 0.4134$$
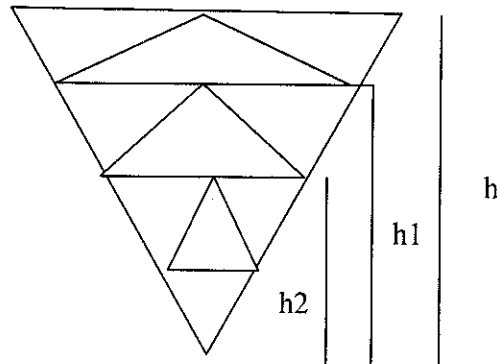
Figure 8   The Sierpinski Gasket heights

The simplified geometry and dimensions of the investigated configuration are depicted in Fig.8.

3.3   CST Software

CST MICROWAVE STUDIO® (CST MWS) from Computer Simulation Technology is a time domain tool capable of analyzing broad-band structures with multiple resonances. It is used to study antenna behaviors. The supporting processing facilities yield to magnitude of interest for an antenna designer, with near field plots, S parameter plot, directivity or far field gain in 3D, polar and xy-plots...

The results are interpreted by S11 response. Scatter Parameters, also called S-parameters, belong to the group to two port parameters used in two port theory, in which, inputs and outputs expressed in power, therefore S-parameters are also transmission and reflection coefficients.
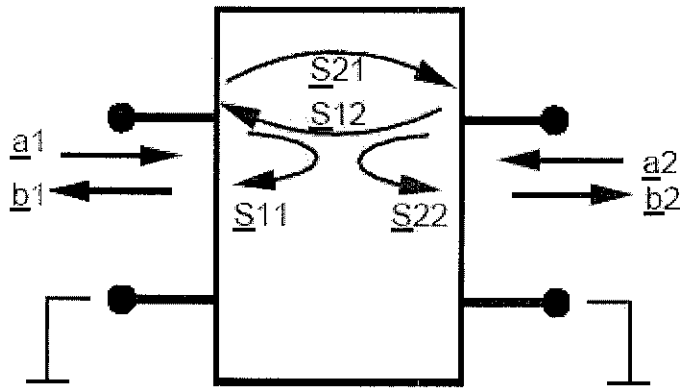
Figure 9   S-parameters

In this project, only one port has been used, therefore only S11 and S21 exist. S11 is equivalent to the input complex reflection coefficient. S21 is the forward complex transmission coefficient.

The simulation result (resonant frequency) should be represented by reflection coefficient S_{11} versus frequency. At the resonant frequency, the reflection coefficient amplitude is in the minimum value. The reason is that at resonant frequency, almost input power is convert to radiation power, leading the reflecting power approximately equals to zero in decimal scale or high negative in dB scale.

3.4   Model Construction in CST Software

The antenna structure was drawn by using the built-in features of CST software. All antenna shape, dimensions, material parameter was chosen or drawn by clicking the appropriate options. In more detail, the shape of antenna was constructs complicated by many triangle shapes, one feeding line and a substrate brick. The material for antenna and ground planes chosen is PEC (perfect electrically conducting), and substrate layer' material is substrate with dielectric constant $\varepsilon_r = 2.2$ and thickness 0.8 mm. The substrate material and thickness was chosen basing on the material which is available and popular in antenna industry. The geometry and dimensions of the investigated configuration are depicted in Fig.10 and 11. It has the dimensions of a PC card whereas the dimensions of the ground plane are 96.6 by 90 mm. The

25

antenna system consists of two metallic layers with the antenna placed at the upper one and the ground plane at the bottom. The thickness of the copper layers is 0.05mm.

The schematic diagram of the proposed antenna is shown in Fig. 10. As shown in Fig. 10, the antenna is fed by a microstrip line like conventional monopole antennas.

By choosing 3 points, the port surface was determined. In this antenna simulation, only one port was established. The 3D structure of the antenna is shown as the figure below.
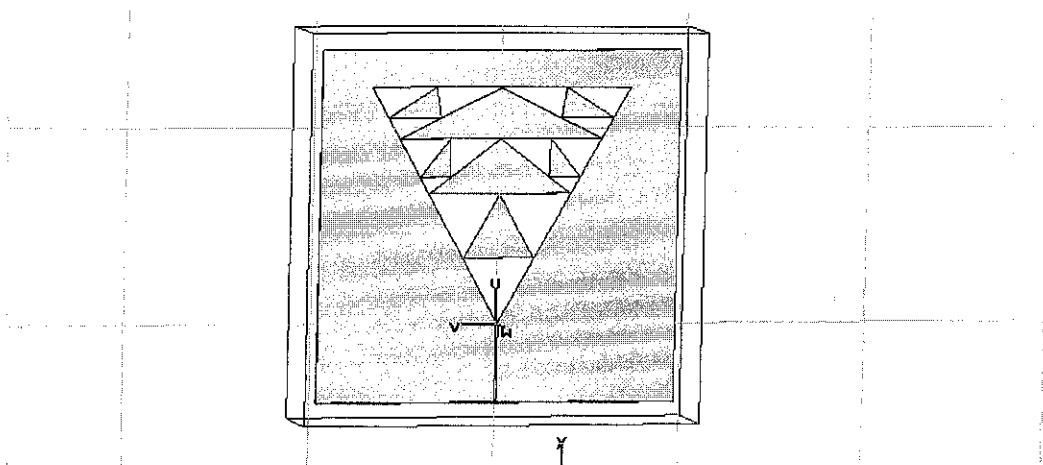

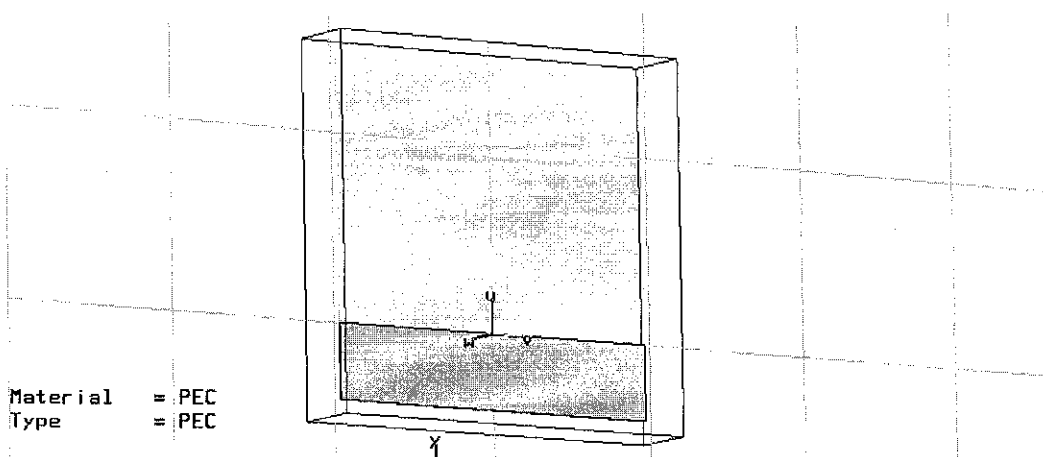Figure 10   The antenna structure (top plane)

Figure 11   The antenna structure (back plane)

3.5 Simulation setting

Some parameters need to set before simulating. Since we interested in the frequency up to 10GHz, the frequency range is set from 0 to 10 GHz. The antenna will be fabricate on the back of a cell phone or the laptop cover, the boundary conditions are set extra open for the place facing to the atmosphere and set to open to the other plane. Mesh properties which define how many mesh boxes to calculate, the more mesh lines are set, the more accurate the result is. In this simulation, the mesh properties were set to generate automatically to find an optimal mesh.

Since the amount of data generated by a broadband time domain calculation is huge, it is necessary to define which field data should be stored before simulation is started. In this case, the farfield monitors for each frequency are stored.

Another important simulation setting is the accuracy. The accuracy setting is to control the numerical truncation errors introduced by the finite simulation time interval. The transient solver calculates the time varying field distribution in the device which results from excitation with a Gaussian pulse at the input port as the primary results. If the accuracy of the time signals is extremely high, numerical inaccuracies can be introduced by the Fourier Transform which assumes that the time signals have completely decayed to zero at the end. The level of truncation error can be controlled by using the Accuracy setting in the transient solver box. The default value is -30dB. To obtain higher accurate results, the accuracy can be set higher such as -40 db or -50 dB. Since increasing the accuracy requirement for the simulation limits the truncation error, and thus increases the simulation time, it should be specified with care. If the no or small ripple in S parameters, the result is considered acceptable.

27

CHAPTER 4

RESULTS AND DISCUSSIONS

4.1 Results and Discussions

According to the theoretical parameters in design for three different frequency bands 2.4 GHz, 3.5 GHz, 5.8 GHz, the simulation results are presented in figure 12.
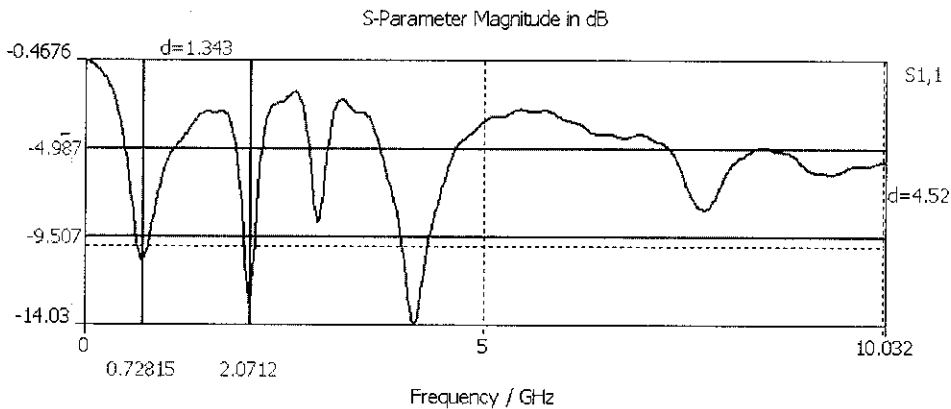

Figure 12   S11 response for the theoretical design setting.

As mention earlier, the S11 value or reflection coefficient will show how much power antenna radiates reflect back. Therefore the less power reflects or more negative value of S11, the more effectively antenna radiates. On the figure 12, S11 curve, the x-axis shows the frequency in GHz, and the y- axis is the S11 value in dB. Basing on this principle, from the figure 12, the fractal antenna performs more effectively within the frequency bands which allocated at 0.72815 GHz, 2.0712 GHz, 2.9126 GHz and 4.1424 GHz.

From that, there are some mismatches between the theoretical values and simulation

values. The mismatches between theoretical design and simulation results are caused since all values are calculated approximately. The other reason is the lost of the similarity of the Sierpinski structure. As well known the frequency ratio between first two bands is 3.5. The modification truncated the infinite ideal fractal structure. When the height of sub-triangles are varied accordingly the allocated frequency bands, the similarity in structure and infinite iteration in traditional Sierpinski Gasket are broken. That is why the band location shifted as shown in figure 12.

As discussing the way to adjust band allocations, by turning the height of each sub-triangle, the frequency bands were allocated exactly as 2.4 GHz, 3.5 GHz and 5.8 GHz, which were shown in figure 13. The values of S11 at each frequency are smaller than -10dB, the threshold value to indicate antenna radiates effectively.
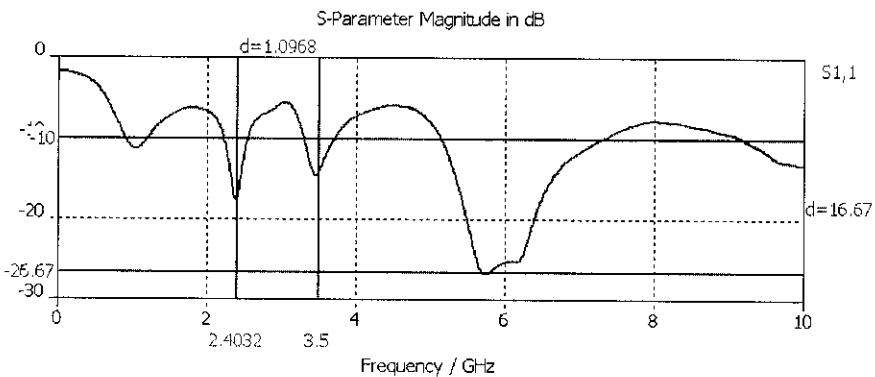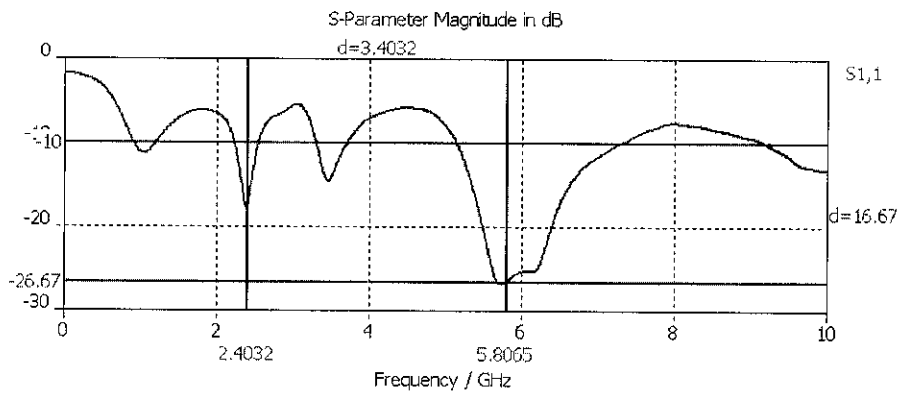

Figure 13   S11 response for the tuning setting to 2.4 GHz, 3.5 GHz, 5.8 GHz.

29

The bandwidth of the resonant frequency is determined by 3dB in S11 larger than the S11 value at the resonant frequency. Therefore the bandwidth of each resonant frequency was summarized as bellowing:

Resonant frequency (GHz)	Bandwidth (MHz)
2.4	136.2 (2.3263GHz-2.4625 GHz)
3.5	285 (3.3436 GHz -3.6286 GHz)
5.8	681 (5.5951 GHz -6.2761 GHz)

From the above table, one interesting point is that the frequency band at 5.8GHz is a broadband.

The far-field plot (fig.14, 15, 16) shows the radiation patterns and the direction which the antenna radiates most effectively.
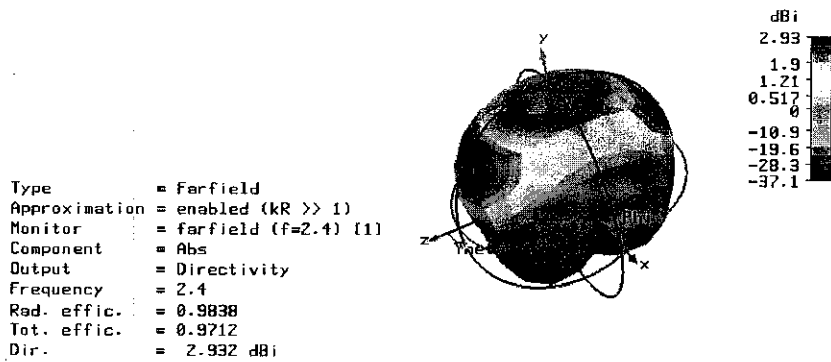


```
Type            = Farfield
Approximation   = enabled (kR >> 1)
Monitor         = farfield (f=2.4) [1]
Component       = Abs
Output          = Directivity
Frequency       = 2.4
Rad. effic.     = 0.9838
Tot. effic.     = 0.9712
Dir.            = 2.932 dBi
```
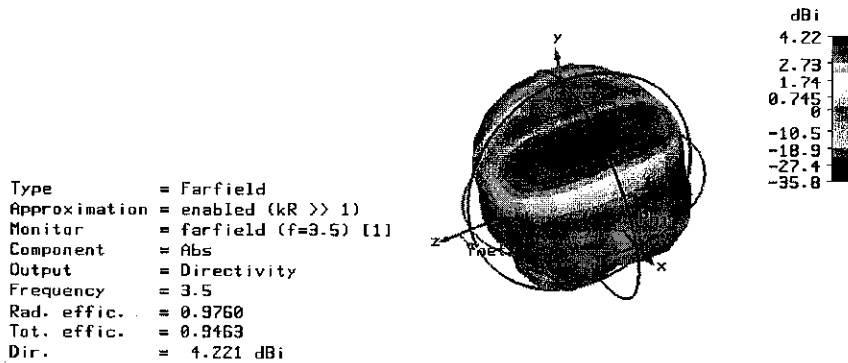
Figure 14   The Farfield response in 3D at 2.4 GHz


```
Type            = Farfield
Approximation   = enabled (kR >> 1)
Monitor         = farfield (f=3.5) [1]
Component       = Abs
Output          = Directivity
Frequency       = 3.5
Rad. effic.     = 0.9760
Tot. effic.     = 0.9463
Dir.            = 4.221 dBi
```

Figure 15   The Farfield response in 3D at 3.5 GHz

```
dBi
5.36
3.47
2.21
0.947
0
-10.2
-18.3
-26.5
-34.6
```

Type   = Farfield
Approximation = enabled (kR >> 1)
Monitor   = farfield (f=5.8) [1]
Component   = Abs
Output   = Directivity
Frequency   = 5.8
Rad. effic.   = 0.9826
Tot. effic.   = 0.9822
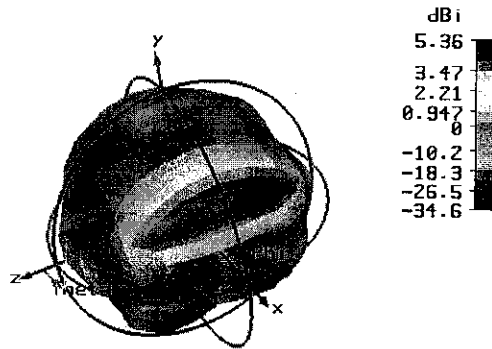Dir.   = 5.364 dBi

Figure 16   The Farfield response in 3D at 5.8 GHz

The farfield in 3D describes the radiation pattern in 3 dimensions. Thanks to that, the direction which the antenna radiates most effectively was determined easily by the gain value (in dB) in such direction. The radiation patterns are symmetric via the antenna plane as expected for a standard monopole antenna. The simulated gain is 2.93 dB, 4.22 dB, 5.36 dB at 2.4 GHz, 3.5 GHz and 5.8 GHz respectively. At the frequency of 5.8 GHz, the antenna radiates more effectively than other frequencies.

Fig. 17, 18, shows the input impedance $Z = R + j X$ as a function of frequency, for various parasitic. Since the antenna equivalent model contains inductance and capacitance, the total impedance of the antenna is depended on frequency.

Real Part of Z Matrix Coefficients in V/A

d= 1.0806

Z1,1

489.9

400

300

200

120.6
100

90.45
30.28

d=30.15

1.5806   2   2.4032   3   3.4839   4   4.4677

Frequency / GHz

Real Part of Z Matrix Coefficients in V/A

5.8

Z1,1

489.9

400

300

200

100

30.28

Z1,1 : 94.67
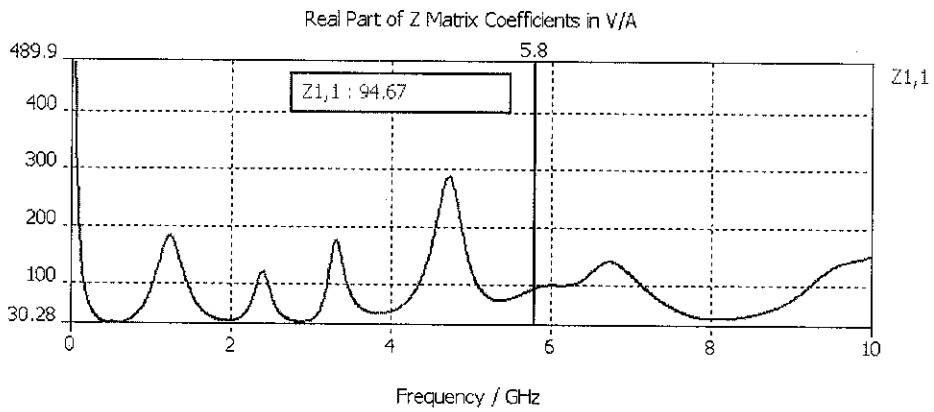
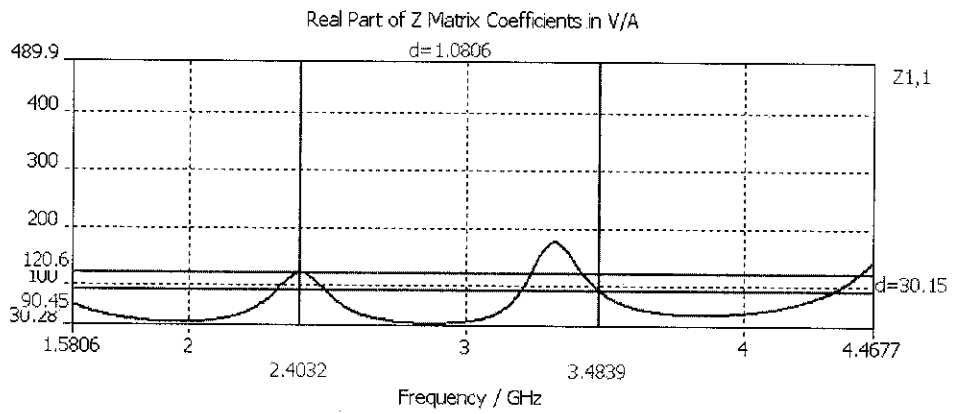0   2   4   6   8   10

Frequency / GHz

Figure 17   The real part of antenna impedances at 2.4 GHz and 3.5 GHz and
5.8 GHz

32

Imaginary Part of Z Matrix Coefficients in V/A

115.6 | 2.4032 | Z1,1
Z1,1 : 0.8791
0
-100
-137.7
1.871 2   2.5   3   3.4677

Frequency / GHz

Imaginary Part of Z Matrix Coefficients in V/A

115.6 | 2.6694 | Z1,1
Z1,1 : -18.01
0
-100
-137.7
1.871 2   2.5   3   3.4677

Frequency / GHz

Imaginary Part of Z Matrix Coefficients in V/A

200 | 5.8 | Z1,1
100
Z1,1 : 2.886
0
-100
-200
-300
-400
-500
-600
0   2   4   6   8   10
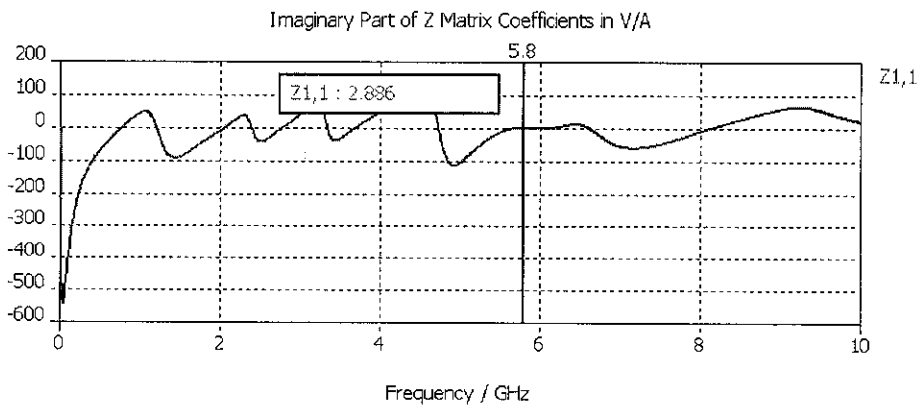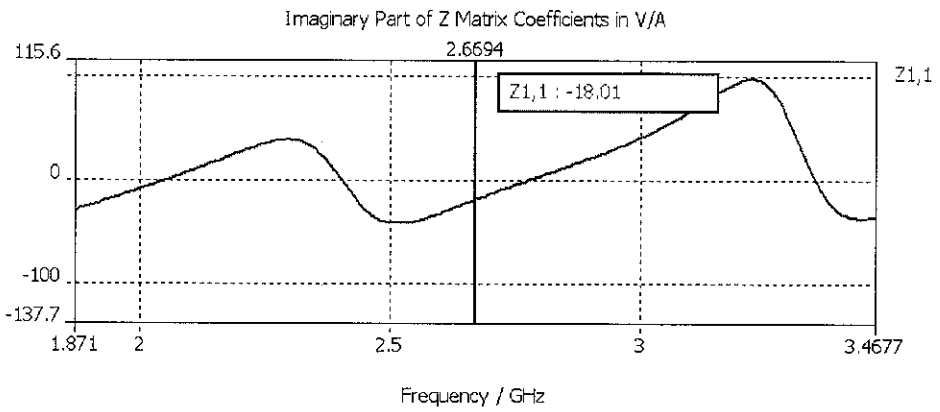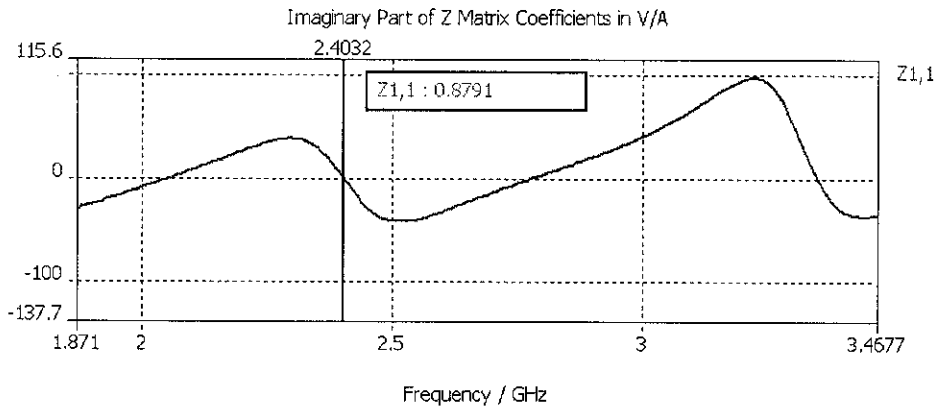
Frequency / GHz

Figure 18   The imaginary part of antenna impedances at 2.4 GHz and 3.5 GHz , and 5.8GHz

The impedances for each frequency are summarized in the following table:

Frequency band (GHz)	$Z = R + j\,X$ *(Ohm)*
2.4	$120.6 + j0.8791$
3.5	$90.45 - j18.01$
5.8	$94.67 + j2.886$

Table 2   The impedance for each frequency

Added to that, the design is very flexible since the band allocation can be adjusted as required. When the height h2 is increase, the third band frequency will move to the left side that means lower frequency. By that principle, some tri-band designs are obtained:
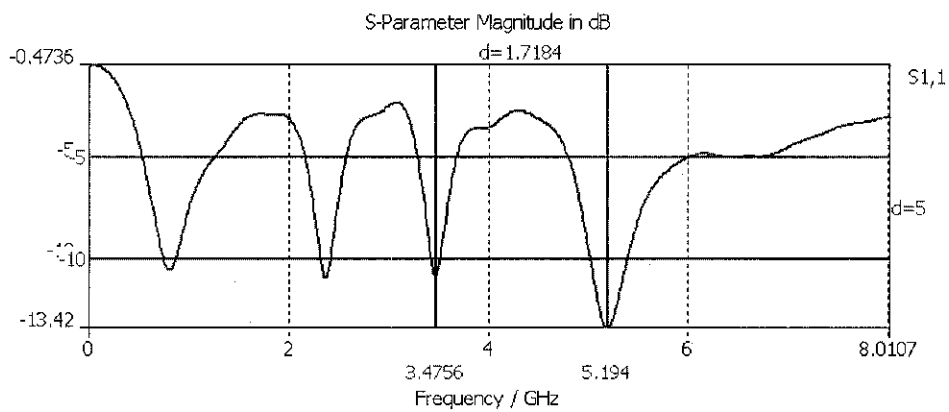

Figure 19   S11 response show the operating frequency bands at 2.4 GHz, 3.5GHz and 5.2 GHz. (h=59; h1=0.782*h; h2=0.55*h)

S-Parameter Magnitude in dB
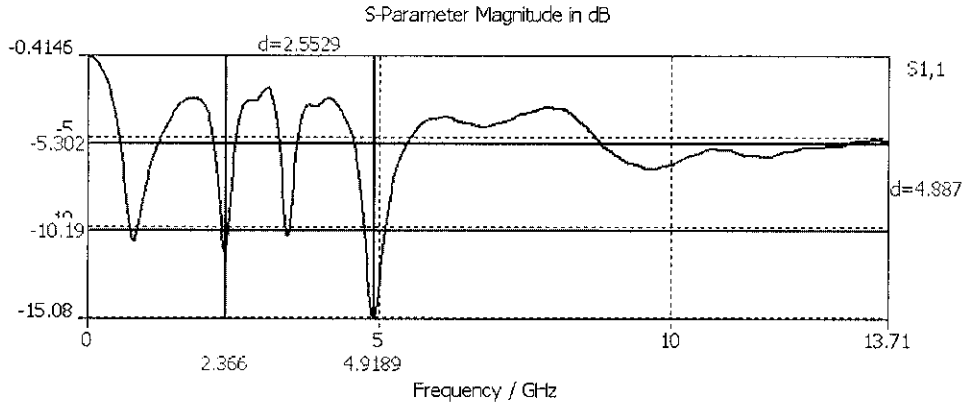

Figure 20 S11 response show the operating frequency bands at 2.4 GHz, 3.5GHz and 5 GHz. (h=59; h1=0.787*h; h2=0.56*h)

4.2 Design Modifications

As mentioning previously, the first and second frequency ration is fixed to 3.5 for conventional Sierpinski antenna. The first frequency decides the size of the antenna. To reduce the size of the Sierpinski fractal antenna, one technique which can be derived logically, is by changing the fixed ratio 3.5. In previous discussion, the band allocations are mismatched with the theoretical design may be caused by the broken of the similarity structure. The motivation for the modified configuration originated from the fact that at the first band of the Sierpinski monopole gasket the similarity and periodicity is lost due to the truncation effect from the finite number of iterations. Since the similarity is lost one can take advantage of it by altering the geometry of the upper subscale in an effort to change the electromagnetic behavior and control the spacing between the first two bands. One way to destroy the similarity is omitting some triangles. As it illustrates by the new design configuration, the new simulation was set up with the parameter as below:
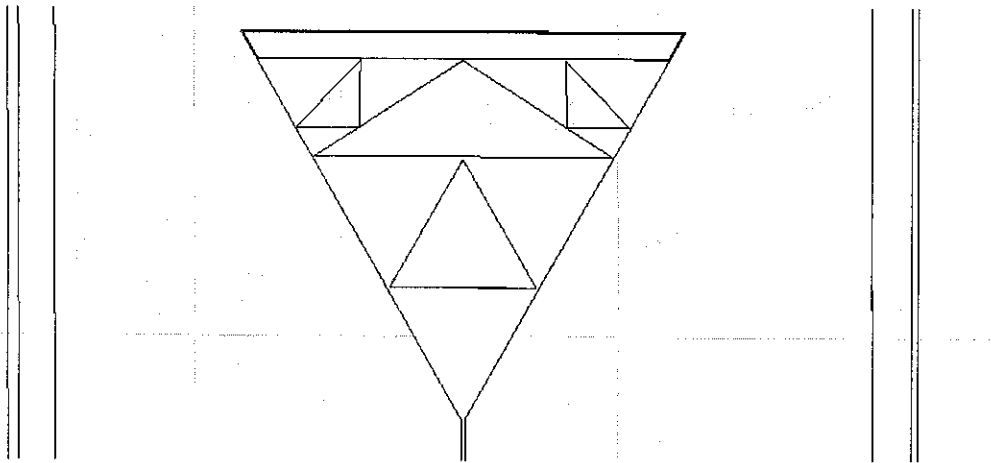
h=45.5

h1=0.93*h

h2= 0.68*h

Figure 21   The modified fractal antenna
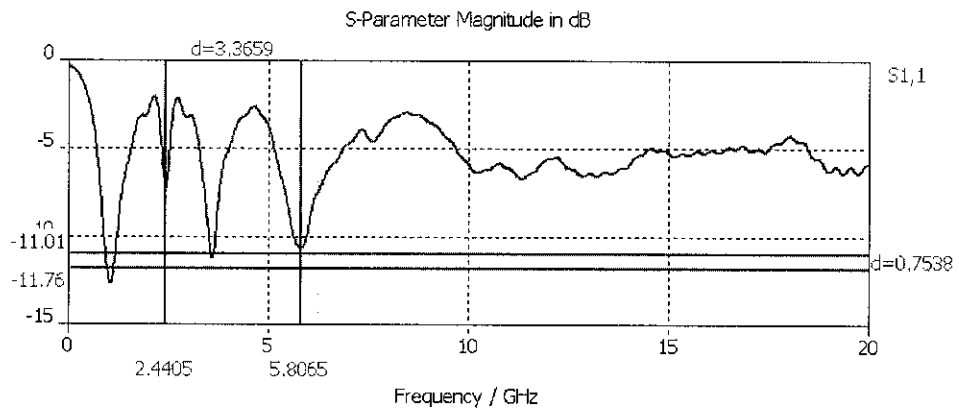

Figure 22   S11 response show the operating frequency bands at 2.4 GHz, 3.5GHz and 5.8 GHz. (h=45.5; h1=0.93*h; h2=0.68*h)

From fig.23, 24, the size of the antenna, h reduces from 59mm to 45.5mm, however the operating frequency bands remain the same. Therefore by omitting some sub-triangles, the similarity structure is broken, leading the frequency ratio at the first and 2nd frequency is smaller than 3.5-the ratio of the traditional Sierpinski fractal shape, consequently, the size of the antenna is reduced.

CHAPTER 5

CONCLUSSIONS AND RECOMMENDATIONS

5.1 Conclussions

The purpose of this project was to present design issues for multi-band and sized-reduced antennas in a hand-held environment. The potential candidates for small and low-profile structure antenna are fractal antennas, especially Sierpinski fractal antennas. At market nowadays, the multi-band antennas are planar inverted-F antennas (PIFA) and IFA since they are easier to many frequency band design (by combining many IFA or PIFA in one) and large gain. However, they are more difficult in manufacturing bigger in size than microstrip antennas (because of their 3D structure) and only dual frequency band antennas were introduced. The proposed antenna was simulated successful radiating in tri-band of frequencies at 2.4 GHz (136.2 MHz), 3.5 GHz (285 MHz) and 5.8 GHz (681 MHz).

Theoretical models on these fractal printed monopole antennas were investigated chapter 2. Then chapter 3 presented the technique used to design the antenna. The more detail about the proposed antenna behaviors were discussed in chapter 4.

The modified Sierpinski gasket monopole antenna printed on the circuit board of a tri- band wireless device has been presented. The modified Sierpinski gasket is an efficient radiator with the ability to allocate both the 2.4 and 3.5 and 5.8 GHz bands. The modification presented in this project achieved by controlling the heights of the Sierpinski Gasket and its sub-triangles basing on Sierpinski Gasket characteristics. The design can applied variously in WiFi and WiMax industry since its small size and easy to fabricate in large amount.

5.2 Recommendations

Within two semesters, the project achievements are still limited. The project opens further study on reducing size study. There are many ways to break the similarity of the fractal Sierpinski antenna. For different frequency, the antenna impedance corresponds differently. Thus it is necessary to have the matching network to optimize power transmission for each frequency band. Moreover, some improvements can be carried out in issues such as radiation efficiency, radiation directions, and a prototype should be fabricate to verify the simulation results.

REFERENCES

[1] Ramesh Garg Et Al, Microstrip Antenna Design Handbook, Chapter 1, Artech House, 2001.

[2] B.B. Mandelbrot, The Fractal Geometry Of Nature, W.H. Freeman, New York, 1983.

[3] Nemanja Popržen And Mićo Gaćanović, Fractal Antenna: Design, Characteristic, And Application, Regular Paper, Phd Seminar "Computational Electromagnetics And Technical Applications", Bosnia And Herzegovina, 2006.

[4]   Http://Www-Tsc.Upc.Es/Eef/Research_Lines/Antennas/Fractals/History.Html (accessed date: 15-05-2007)

[5] G. A. Edgar, *Measure, Topology, and Fractal Geometry*. New York: Springer-Verlag, 1990, ch. 1.

[6] C. Puente, J. Romeu, R. Pous, And A. Cardama, "On The Behavior Of The Sierpinski Multiband Fractal Antenna," *IEEE Trans. Antennas Propagat.*, Vol. 46, Pp. 517–524, Apr. 1998.

[7] C. Puente, J. Romeu, R. Bartoleme, And R. Pous, "Perturbation Of The Sierpinski Antenna To Allocate Operating Bands," *Electron. Lett.*, Vol. 32, No. 24, Pp. 2186–2188, Nov. 1996.

[8] D. L. Jaggard, "Fractal Electrodynamcis: From Super Antennas To Superlattices," Pp. 204 - 221 In *Fractals In Engineering*, Vehel, Lutton And Tricot, Editors, Springer-Verlag, Berlin (1997).

[9] George F. Tsachtsiris, Constantine F. Soras, Manos P. Karaboikis, Vassilios T. Makios, 'Analysis Of A Modified Sierpinski Gasket Monopole Antenna Printed On

Dual Band Wireless Devices', Ieee Transactions On Antennas And Propagation, Vol.
52, No. 10, Octobber 2004

APPENDICES

APPENDIX A

S- PARAMETER

<u>Review of Scattering Matrix</u>

1)   Normalization with respect to $\sqrt{Z_o}$ of wave amplitudes:

$$a = \frac{V^+}{\sqrt{Z_o}} \text{ and } b = \frac{V^-}{\sqrt{Z_o}} \text{ , so power is } aa^* \text{ and } bb^*$$

2)   Relationship of b_n and a_n: $b_n = \Gamma_n a_n$

3)   Expressions for b_1 and b_2 at reference planes:

$$b_1 = S_{11}a_1 + S_{12}a_2$$
$$b_2 = S_{21}a_1 + S_{22}a_2$$

4)   Definitions of S_{ij}:

$$S_{11} = \frac{b_1}{a_1} \text{ for } a_2 = 0, \text{ i.e., input } \Gamma \text{ for output terminated in } Z_o.$$

$$S_{21} = \frac{b_2}{a_1} \text{ for } a_2 = 0, \text{ i.e., forward transmission ratio with } Z_o \text{ load.}$$

$$S_{22} = \frac{b_2}{a_2} \text{ for } a_1 = 0, \text{ i.e., output } \Gamma \text{ for input terminated in } Z_o.$$

$$S_{21} = \frac{b_1}{a_2} \text{ for } a_1 = 0, \text{ i.e., reverse transmission ratio with } Z_o \text{ source.}$$

$|S_{21}|^2$ = Transducer power gain with Z_o source and load.

5)   Definitions of Γ_L, Γ_s, Γ_{in} and Γ_{out}:

$$\Gamma_L = \frac{Z_L - Z_o}{Z_L + Z_o} \text{ , the reflection coefficient of the load}$$

$$\Gamma_s = \frac{Z_s - Z_o}{Z_s + Z_o} \text{ , the reflection coefficient of the source}$$

$$\Gamma_{in} = \frac{Z_{in} - Z_o}{Z_{in} + Z_o} = S_{11} + \frac{S_{12}S_{21}\Gamma_L}{1 - S_{22}\Gamma_L} \text{ , the input reflection coefficient}$$

$$\Gamma_{out} = \frac{Z_{out} - Z_o}{Z_{out} + Z_o} = S_{22} + \frac{S_{12}S_{21}\Gamma_s}{1 - S_{11}\Gamma_s} \text{ , the output reflection coefficient}$$

6)   Power Gain G, Available Gain G_A, Transducer Gain G_T:

$$G = \frac{P_L}{P_{in}} = \frac{\text{power delivered to the load}}{\text{power input to the network}}$$

$$G_A = \frac{P_{avout}}{P_{avs}} = \frac{\text{power available from the network}}{\text{power available from the source}}$$

$$G_T = \frac{P_L}{P_{avs}} = \frac{\text{power delivered to the load}}{\text{power available from the source}}$$

Power Gain Equations

The equations for the various power gain definitions are

1) $G = \dfrac{P_L}{P_{in}} = \dfrac{1}{1 - |\Gamma_{in}|^2} \, |S_{21}|^2 \, \dfrac{1 - |\Gamma_L|^2}{|1 - S_{22}\Gamma_L|^2}$

2) $G_A = \dfrac{P_{avout}}{P_{avs}} = \dfrac{1 - |\Gamma_s|^2}{|1 - S_{11}\varpi_s|^2} \, |S_{21}|^2 \, \dfrac{1}{1 - |\Gamma_{out}|^2}$

3) $G_T = \dfrac{P_L}{P_{avs}} = \dfrac{1 - |\Gamma_s|^2}{|1 - \Gamma_{in}\Gamma_s|^2} \, |S_{21}|^2 \, \dfrac{1 - |\Gamma_L|^2}{|1 - S_{22}\Gamma_L|^2}$

$\qquad\qquad = \dfrac{1 - |\Gamma_s|^2}{|1 - S_{11}\Gamma_s|^2} \, |S_{21}|^2 \, \dfrac{1 - |\Gamma_L|^2}{|1 - \Gamma_{out}\Gamma_L|^2}$

The expressions for Γ_{in} and Γ_{out} are

1) $\Gamma_{in} = S_{11} + \dfrac{S_{12}S_{21}\Gamma_L}{1 - S_{22}\Gamma_L}$

2) $\Gamma_{out} = S_{22} + \dfrac{S_{12}S_{21}\Gamma_s}{1 - S_{11}\Gamma_s}$

For a unilateral network, $S_{12}=0$ and

1) $\Gamma_{in} = S_{11}$ if $S_{12}=0$ (unilateral network)

2) $\Gamma_{out} = S_{22}$ if $S_{12}=0$ (unilateral network)

The transducer gain G_T can be expressed as the product of three gain contributions

$G_T = G_s G_o G_L$, where

$G_o = |S_{21}|^2$

$G_s = \dfrac{1 - |\Gamma_s|^2}{|1 - \Gamma_{in}\Gamma_s|^2}$ and